



THE UNIVERSITY *of* EDINBURGH

Edinburgh Research Explorer

Robust self-scheduling of a price-maker energy storage facility in the New York electricity market

Citation for published version:

Barbry, A, Anjos, MF, Delage, E & Schell, KR 2019, 'Robust self-scheduling of a price-maker energy storage facility in the New York electricity market', *Energy Economics*, vol. 78, pp. 629-646.
<https://doi.org/10.1016/j.eneco.2018.11.003>

Digital Object Identifier (DOI):

[10.1016/j.eneco.2018.11.003](https://doi.org/10.1016/j.eneco.2018.11.003)

Link:

[Link to publication record in Edinburgh Research Explorer](#)

Document Version:

Peer reviewed version

Published In:

Energy Economics

General rights

Copyright for the publications made accessible via the Edinburgh Research Explorer is retained by the author(s) and / or other copyright owners and it is a condition of accessing these publications that users recognise and abide by the legal requirements associated with these rights.

Take down policy

The University of Edinburgh has made every reasonable effort to ensure that Edinburgh Research Explorer content complies with UK legislation. If you believe that the public display of this file breaches copyright please contact openaccess@ed.ac.uk providing details, and we will remove access to the work immediately and investigate your claim.



Robust self-scheduling of a price-maker energy storage facility in the New York electricity market

Adrien Barbry^{a,c}, Miguel F. Anjos^{a,c,*}, Erick Delage^{b,c}, Kristen R. Schell^{a,c}

^a*Department of Mathematics and Industrial Engineering, Polytechnique Montréal (Québec), Canada*

^b*Department of Decision Sciences, HEC Montréal (Québec), Canada*

^c*GERAD, Montréal (Québec), Canada*

Abstract

Recent progress in energy storage raises the possibility of creating large-scale storage facilities at lower costs. This may bring economic opportunities for storage operators, especially via energy arbitrage. However, storage operation in the market could have a noticeable impact on electricity prices. This work aims at evaluating jointly the potential operating profit for a price-maker storage facility and its impact on the electricity prices in the New York state market. Based on historical data, lower and upper bounds on the supply curve of the market are constructed. These bounds are used as an input for the robust self-scheduling problem of a price-maker storage facility. Our computational experiments show that the robust strategies thus obtained allow to reduce significantly the loss exposure while maintaining reasonably high expected profits.

Keywords: energy storage, electricity market, bidding strategy, arbitrage, quantile regression, robust optimization

1. Introduction

Over the last five years, great progress has been achieved in the field of energy storage. Among the different technologies of energy storage, this progress has been especially significant in the field of batteries. A few years ago, provided their limited power and energy capacity, batteries were mainly considered as a mean to support renewables, damping the variability of wind and PV systems [1]. The recent deployment of large-scale batteries, exemplified by the 70 MW system brought online in California in late 2016 [2], heralds new potential applications for batteries. As of February 15,

*Corresponding author

Email address: miguel-f.anjos@polymtl.ca (Miguel F. Anjos)

2018, the Federal Energy Regulatory Commission (FERC) has mandated that RTOs/ISOs modify their market policies to allow energy storage to participate in wholesale markets as a price maker, when either buying or selling energy [3]. FERC further mandates that storage operators as small as 100kW must be allowed to bid into these markets. Given these changes in market regulation, as well as the technological advancement and cost reductions associated with greater storage deployment, one might anticipate that storage will indeed become an influential price maker in the near future.

The deregulation of the electricity sector in many regions has led to the emergence of wholesale electricity markets and thus created economic opportunities for energy storage [4]. The price volatility on these markets is indeed a potential source of profit for energy storage facilities, which can buy (and store) electricity during periods of low demand (and low prices) and sell it back to the grid during periods of high demand (and high prices). This type of opportunity in the market is referred to as energy arbitrage. Other applications exist and may be profitable for energy storage, such as ancillary services, and operating reserve [5].

In this paper, we focus on energy arbitrage. This is one of the best understood and more interesting applications in volatile markets. Such opportunities are especially present in New York's day-ahead electricity market (DAM), which will be the focus of our study. Figure 1a shows the evolution of the hourly price in 2016. Over the span of this year, the prices ranged between \$0.01/MWh and \$93.23/MWh. One can also observe a total of 1000 hours when a price lower than \$8.85/MWh was reached, and 1000 hours with prices greater than \$32.55/MWh. The daily difference between off-peak price and peak-price is illustrated in Figure 1b: this highlights the daily frequency of opportunities for energy arbitrage.

As a result of these opportunities, the energy storage sector is likely to attract investment in the years to come. However, investing in such large-scale facilities requires an accurate evaluation of the potential benefits of energy arbitrage. One possibility to assess the profits of a large-scale energy storage facility is to determine what would have been an optimal operating plan during the past years and compute the associated profit. This consists in formulating the optimal hourly bids for each day. In practice, in energy markets, the bids are classified into two types: self-schedule bids and economic bids [6]. A self-schedule bid does not include a price component: it indicates that the participant is willing to buy/sell electricity regardless of the price. An economic bid does include a price component: it indicates that the participant is willing to buy/sell electricity provided that the cleared market price is at most/at least the submitted price bid. In the case of energy

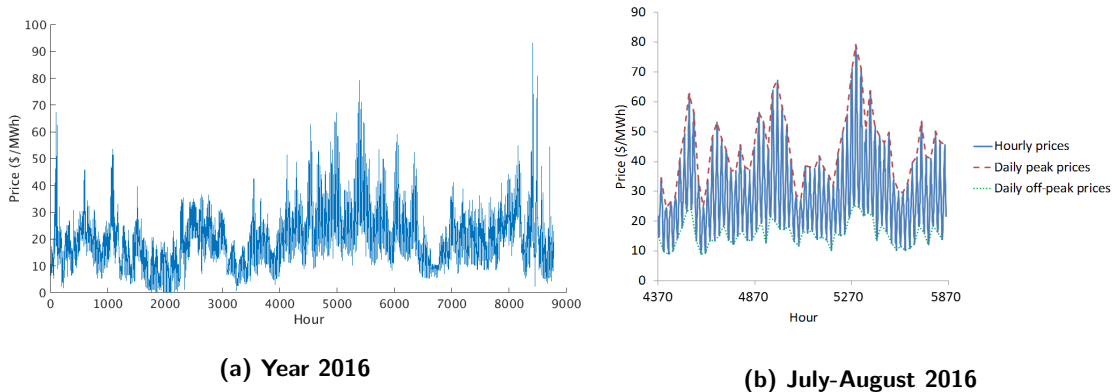


Figure 1: Hourly electricity prices in NY day-ahead market

storage, the self-scheduling formulation is generally preferred [7, 4, 8], because the hourly bids are
 40 interdependent. For instance, the storage operator needs to be certain that his purchase bids have
 been accepted so that he can sell this electricity later.

Many studies have been conducted to assess the profitability of energy storage facilities doing
 energy arbitrage in different electricity markets. Different storage technologies are considered in
 these studies, but storage facilities are generally characterized by three main features regardless of
 45 the technology: the power capacity (in MW), the energy capacity (typically given in MWh), and
 an efficiency quantifying the losses incurred during both charging and discharging operations. The
 energy capacity of a storage device may also be seen as the number of hours of full power output.
 These studies may be divided in two categories depending on the power capacity of the energy
 storage facility.

50 The first category assumes that the energy storage facilities are price-takers, which means that
 their operation does not significantly affect the market price. This is generally the case when the
 storage power capacity is small compared to the total demand or supply in the market, so that
 the demand or supply is not affected by the storage operation. The value of small energy storage
 devices in two jurisdictions of the US, PJM and New York state (NY) are estimated in [4] and [9]
 55 respectively. [4] examines the effect of two parameters on the value of storage (efficiency and energy
 capacity) and establishes that this value may range from \$60/kW-year to \$120/kW-year depending
 on these parameters. The impact of the price of fuel (natural gas and coal) on the value of arbitrage
 is also highlighted: hourly on-peak prices are often set by natural gas or coal generation, therefore

increases in the price of commodities lead to increases in the value of storage. [9] underlines the economic opportunity in NY for energy storage installations, and compares the economics of two technologies (sodium sulfur batteries and flywheel). The resulting revenues are comparable with those in PJM. In [10], Sioshansi et al. explore the value drivers behind energy arbitrage for two different technologies (pumped-hydro storage and compressed air storage). In particular, it is shown that, due to its hybrid nature, compressed air storage is more sensitive to gas price fluctuations. A model is proposed in [11] to optimize the schedule of energy storage devices participating in both energy and reserve markets in different regions of the USA. The combination of energy arbitrage and operating reserve increase the value of energy storage in some markets. Finally, Wang et al. propose a novel framework in [12] to optimize the bidding strategy of a storage unit considering both the day-ahead and the following day markets. A special emphasis is put on the determination of the optimal state of charge at the end of the day-ahead.

This first set of studies provides a picture of the arbitrage value of energy storage in different markets. However, these studies assume that the storage operation does not affect the market price, which is a valid assumption provided that the storage capacity is sufficiently small. Our study focuses on larger-scale facilities, which may affect more significantly the demand and supply on the market when they operate. Charging during low-demand periods and discharging during peak periods will reduce the price gap, and therefore the arbitrage value. In this case, the energy storage facility becomes price-maker. To accurately assess the potential profits of a large-scale energy storage facility, it is essential to account for the impact of storage operation on the price.

A few studies have addressed the self-scheduling of a large-scale energy storage facility [7, 4, 13, 8]. The general idea is to describe, at each time step, the market price p_t as a non-increasing function of the quantity q_t submitted by the energy storage on the market, i.e. $p_t = f_t(q_t)$, where q_t can either be positive (when discharging) or negative (when charging). The variable t refers to the time slicing of the market, according to the frequency with which the bids are formulated. In the case of the day-ahead market, bids have to be formulated on an hourly basis. For the sake of simplicity, it is convenient to express q_t as the difference of two non-negative variables: $q_t = P_t^d - P_t^c$ where P_t^d is the discharging power and P_t^c is the charging power at time step t . Based on these variables, the energy level of the storage E_t at each time step t can be computed. Hence, the self-scheduling problem may be formulated as follows:

$$\max_{\{P_t\}_{t=1}^T, \{E_t\}_{t=1}^{T+1}} \sum_{t=1}^T (P_t^d - P_t^c) f_t(P_t^d - P_t^c) - \sum_{t=1}^T C(P_t^d + P_t^c) \quad (1a)$$

$$\text{subject to} \quad 0 \leq P_t^d \leq P_{max}^d \quad \forall t \in \llbracket 1, T \rrbracket \quad (1b)$$

$$0 \leq P_t^c \leq P_{max}^c \quad \forall t \in \llbracket 1, T \rrbracket \quad (1c)$$

$$E_{t+1} = E_t + \eta P_t^c - \frac{1}{\eta} P_t^d \quad \forall t \in \llbracket 1, T \rrbracket \quad (1d)$$

$$0 \leq E_t \leq E_{max} \quad \forall t \in \llbracket 1, T+1 \rrbracket \quad (1e)$$

$$E_1 = E_{T+1}, \quad (1f)$$

where $\llbracket 1, T \rrbracket$ denotes all the integers between 1 and T .

90 The objective function (1a) describes the profit of the storage operator. The first part computes the revenues from selling electricity to the market minus the costs from buying electricity from the market. The operating costs of the facility are subtracted in the second part of the objective function: C corresponds to the marginal cost due to operation and degradation during the hours of charging and discharging. These revenues and costs are summed for each hour of the horizon, 95 since the day-ahead market requires hourly bids. Constraints (1b), (1c) and (1e) describe the limits of storage in terms of power capacity and energy capacity. Constraint (1d) computes the state of charge of the storage at each period of time. The losses during both charging and discharging are taken into account by means of an efficiency η . Here we assume the same charging and discharging efficiency, as we model lithium-ion batteries for which this assumption holds [14]. However, it would 100 be easy to incorporate different charging/discharging efficiencies in this model for different types of batteries, should it be desirable to the storage operator. The initial and final state of charge are specified in (1f).

It is worth noting that our model assumes that both a charge and discharge bid can be submitted to the market for the same hourly period. This is without loss of generality as we demonstrate in 105 Appendix 6.1 that this problem always identifies an optimal solution that avoids submitting charge at discharge bids for the same period, i.e. all optimal solutions satisfy the additional non-linear constraint: $P_t^c P_t^d = 0$ for all t .

Two main methods have been proposed in the literature to model the function f_t describing the impact of storage operation on the price. In both cases, it is necessary to understand the price 110 formation process. For each hour, suppliers and consumers submit bids (which are composed of a

quantity, and a price) to the market. After collecting and sorting all these bids, a supply curve and a demand curve may be constructed. The price is then given by the intersection between the two curves.

The first method is the most general, and uses the residual demand curve, which is defined as
115 the market demand curve minus the quantity supplied by other participants. It provides a direct relation between the quantity submitted by the energy storage and the resulting market price. [8] and [13] approximate the residual demand curve of the Iberian market by a sigmoid function, and solve the corresponding non-linear self-scheduling problem. This formulation is particularly relevant when the market demand is elastic.

120 In practice, it is often the case that electricity demand can be assumed to be inelastic. It is then sufficient to model the effect of storage operation on price through a supply curve $\pi(d)$, where d is the demand. Hence, the effect of the storage unit can be taken into account through $f_t(q) = \pi(d_t - q)$. Since the storage is self-scheduling, its operation is indeed equivalent to an increase (when charging) or a decrease (when discharging) in the demand. [4] and [7] exploit respectively the supply curve of
125 the Alberta and PJM electricity markets to formulate the self-scheduling problem of a price-maker energy storage. In [4], a linear supply curve is constructed for each month based on historical data of prices and quantities. In [7], actual supply curves from the Alberta market are used for years 2010 to 2014. For each hour, based on the supply curve and the demand, generation price quota curves (GPQC) and demand price quota curves (DPQC) are constructed to model respectively
130 the price impacts of discharging and charging. This stepwise approximation of the supply curve around the value of the demand allows the formulation of a mixed-integer linear program for the self-scheduling problem.

This paper addresses the economic assessment of energy arbitrage opportunities for a large-scale energy storage operator in the day-ahead market of NY. We will assume that at the moment of
135 submitting his bids, while the operator of such a facility has an accurate idea of the hourly electricity demand, he is unaware of the market clearing price and in particular the exact effect of his bid on this price. This represents realistic operating conditions given that such operators would usually be unaware of the bids that will be submitted by other participants, or even of their conditions of operations (e.g. cost of resources, periods of maintenance, etc.). We will instead assume that the
140 operator employs historical observations of electricity demand, market price, and available hourly wind power production to construct an uncertainty model for the potential supply curves, which

consists of a nominal supply curve, a maximal supply curve, and a minimal supply curve. This uncertainty model will be employed by a robust formulation of the self-scheduling problem (1) that will account for the level of aversion the operator has with respect to the possibility of daily losses. It is worth emphasizing that this is in sharp contrast with the approach presented in [7] and [4], which both assume that the supply curve for every hour of the day is exactly known in advance, or equivalently that the operator is insensitive to estimation errors. Furthermore, our approach will model the supply curve as a piecewise linear function which better captures the increasing marginal impact of supply on prices during high demand periods compared to the piecewise constant model employed in [4].

Overall, the contributions of this paper can be summarized as follows:

- We present for the first time a method to characterize the market price uncertainty that a price-maker participant is confronted with when submitting a self-scheduled bid in a day-ahead market. Our approach is based on performing least squares and quantile regressions on historical observations of total demand, market prices, and wind power production.
- We present for the first time a decision model that employs robust optimization to model the risk aversion of an energy storage operator. In particular, the model will control using a budget Γ under which magnitude of perturbation of a nominal daily profit curve is the operator comfortable with the possibility of a financial loss.
- We show that the robust bidding strategy obtained using this model with a budget of uncertainty of two hours ($\Gamma = 2$) allows to reduce the risk of a financial loss (from 3.01% to 1.09% with respect to the nominal strategy), while maintaining the expected profit at a reasonable level (10.8% below the profit obtained with the nominal strategy).

The remainder of the paper is organized as follows. In Section 2, the modelling of the supply curve, and of its variability is described. In Section 3, the robust self-scheduling problem of a price-maker storage facility is developed. In Section 4, the developed model is applied and the robust strategy of the storage operator, as well as its impact on the market prices, are analyzed.

2. Modelling the supply curve in the day-ahead market of NY

The methodology used in this paper, which is based on the construction of the supply curve, requires a good understanding of the organization of the NY electricity markets, as well as a careful

study of the data extracted from this market.

2.1. New York Electricity Markets

In the state of New York, electricity is traded in a number of competitive electricity markets, all of which are administered by the regional transmission organization called New York Independent System Operator (NYISO). The NYISO is also responsible for operating the state's bulk electricity grid, and for long-term planning for the state's electric power system. The electricity grid serves about 20 million people and has historically been required to supply peaks of demand as high as 32 GW in 2015 (see [15]). In comparison, the total power capacity from sources within the state currently reaches 39 GW, with half of the capacity originating from dual fuel power plants (facilities capable of using natural gas in combination with another fossil fuel). The other half of the total capacity is mainly nuclear (14%), hydro (11%), and gas-only (10%) power plants. The NYISO has also ambitious plans for the development of wind and solar power facilities. In particular, a dramatic increase of the wind power capacity occurred over the last 10 years (from 48 MW in 2005 to 1746 MW in 2015).

Among all the markets operated by the NYISO, this article focuses on the energy day-ahead market, which accounts for over 94% of energy exchanges [16]. In this market, energy suppliers and consumers submit economic bids for each hour of the following day. While the price curves for supply and demand are the key factors determining the market prices, the transmission of electricity also plays a noticeable role. Indeed, bottlenecks can occur on the electricity grid if large volumes need to be transmitted to meet demand in a particular zone. Thus, the NYISO employs a nodal pricing scheme, that gives rise to local marginal prices (LMP) for each of the 11 zones of NY. These LMPs are the result of three contributions: the marginal cost of energy (which is uniform over the state), the cost of losses in transmission lines, and a cost related to congestion in the zone considered. Our study will focus on the main contributor to market prices, namely the marginal cost of energy. The reasons for doing so are two-fold. First, we do not address the issue of determining the optimal location for the storage facility. Hence, the most consistent price to take into account is the marginal cost of energy, which is the same statewide. Secondly, to model the price-maker effect of energy storage, we will use a relation between the load (or supply) and the price via the supply curve. Yet the only component of the price which is directly related to the load is the marginal cost of energy: as the load increases, energy sources with increasingly high marginal costs of production

have to be dispatched to meet the demand. On the other hand, the two other contributions of the price are not directly related to the load, but rather to local transmission constraints.

As shown in Figure 2a, our data set consists of a list of historical pairs $\{(p_i, d_i)\}_{i=1}^{N=366 \times 24}$, ranging from January 1st, 2016 to December 31st, 2016, and describing on an hourly basis the market price and corresponding electricity demand observed on the energy day-ahead market supervised by NYISO. One can observe that the supply curve describing the relationship between the demand and the price is subject to high variability. There are indeed many reasons why bids submitted by suppliers might vary from day to day (or even hour to hour):

- marginal costs incurred by each supplier in the market fluctuate depending on the price of commodities such as natural gas, oil, etc.;
- the production capacity of renewable resources is sensitive to meteorological conditions (wind, rainfall, sunshine) ;
- a power plant may become unavailable at times because of maintenance, etc.

It is reasonable to conclude that predicting exactly where the intersection between the supply curve and the inelastic demand curve will occur for any given hour of the day is a very difficult task. Under such conditions, one should employ a representation that accounts for variability in the supply curve when searching for an optimal bidding strategy.

2.2. Constructing a nominal supply curve

We first attempt to identify a nominal representation of the supply curve by employing the least squares method to perform a regression, following the idea proposed in [4]. Specifically, under the assumption that the supply curve has a parametric form $p = \hat{\pi}(d; \delta)$, one can identify the best fit for $\delta \in \mathbb{R}^m$ by solving the following optimization problem :

$$\min_{\delta} (1/N) \sum_{i=1}^N (p_i - \hat{\pi}(d_i; \delta_i))^2 .$$

Figure 2 presents the nominal curves obtained when $\hat{\pi}(d; \delta)$ is chosen to be an affine function (a.k.a. linear regression) and a piecewise linear function with breakpoints at 25.558 and 28.098. Both of these regressions were performed using the software R version 3.2.0 with the “Segmented” package (available online) [17]. This package allows one to determine jointly the optimal breakpoints and

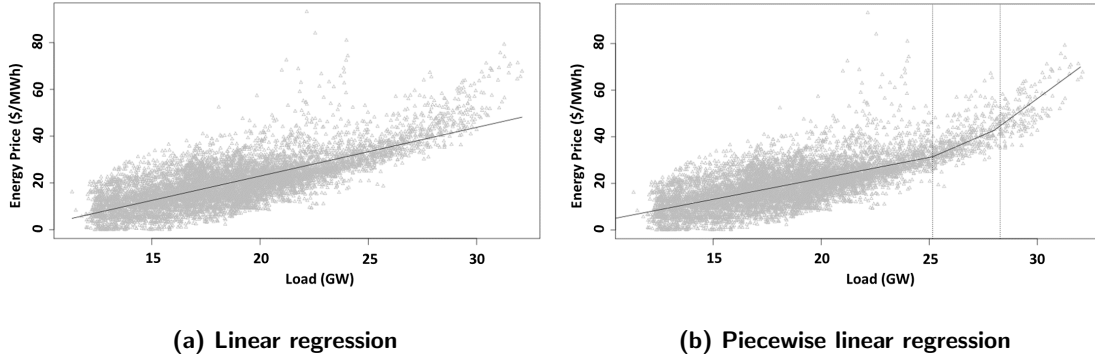


Figure 2: Best fitted models for the nominal supply curve based on historical data $\{(p_i, d_i)\}_{i=1}^N$. (a) presents the calibrated affine function $\hat{\pi}(d; \delta^*)$ with an R^2 of 0.5641. (b) presents the calibrated piecewise linear function $\hat{\pi}(d; \delta^*)$ with an R^2 of 0.5923.

slopes of a piecewise linear function, given that the number of breakpoints is pre-specified. One can also obtain the R^2 statistic of the fitted function which captures the amount of data variability that can be explained by the fitted model. The fact that this statistic increases from 0.5641 to 0.5923 when employing the piecewise linear function confirms that the latter function provides a better fit. We can also expect that the piecewise linear model provides a more accurate description of how the marginal market price can be affected by the magnitude of the demand. This is indeed a key element in the context of the price-maker formulation such as in problem (1) given that it defines the impact that the storage facility will have on the market price.

In order to improve the amount of price variance explained by our nominal model, we also attempted to model the influence of wind variability on the supply curve. In particular, we used the NYISO data about the hourly wind power production $\{(w_i)\}_{i=1}^N$ for each hour of our data set. Since one can usually assume that wind energy has a negligible marginal cost [18], meeting the total demand at the lowest cost is equivalent to meeting the “net demand” (the total demand minus the wind power production) at the lowest cost. For this reason, we perform the same regressions as before but on the modified data set $\{(p_i, n_i)\}_{i=1}^N$ where each $n_i := d_i - w_i$. The resulting linear and piecewise linear regressions produced R^2 statistics of 0.6139 and 0.6485 respectively; increases which support this approach.

The conclusions of this fitting of a nominal supply curve motivate the use of the following

function to model the impact of storage:

$$\hat{f}_t(q_t) := \hat{\pi}(d_t - q_t - w_t; \delta^*) = \hat{\pi}_w(n_t - q_t),$$

240

where

$$\hat{\pi}_w(y) = \begin{cases} 2.086y - 17.354 & \text{if } 0 \leq y \leq 25.558 \\ 4.249y - 72.636 & \text{if } 25.558 < y \leq 28.098 \\ 6.705y - 141.45 & \text{if } 28.098 < y. \end{cases} \quad (2)$$

2.3. Constructing upper and lower bounds for the supply curve

We now turn to the characterization of the variability of the supply curve and the effect of this variability on the cash flows that will be produced when scheduling storage. We use the historical data set $\{(p_i, d_i, w_i)\}_{i=1}^N$ to calibrate two bounding functions $\pi_w^+(n)$ and $\pi_w^-(n)$ so that they return for a given net load n , a confidence interval $[\pi_w^-(n), \pi_w^+(n)]$ for the realized market price. This can be done using quantile regression (as introduced in [19]).

Quantile regression is similar in spirit to the well-known least squares method. One first needs to identify a parametric form for $\pi_w^+(n)$ and $\pi_w^-(n)$, which we will refer to as $\pi_w^+(n; \delta_+)$ and $\pi_w^-(n; \delta_-)$. Given a confidence level α , which we choose to be $\alpha = 10\%$, we will fit the δ_+ and δ_- parameters to the data set $\{(p_i, n_i)\}_{i=1}^N$ but this time using a regression function that aims at capturing the $\alpha/2$ -th and $1 - \alpha/2$ -th quantile respectively. Specifically, the optimization models take the form:

$$\begin{aligned} \delta_-^* &= \arg \min_{\delta_-} (1/N) \sum_{i=1}^N \max \left(\left(1 - \frac{\alpha}{2}\right) (\pi_w^-(n_i; \delta_-) - p_i), \frac{\alpha}{2} (p_i - \pi_w^-(n_i; \delta_-)) \right) \\ \delta_+^* &= \arg \min_{\delta_+} (1/N) \sum_{i=1}^N \max \left(\frac{\alpha}{2} (\pi_w^+(n_i; \delta_+) - p_i), \left(1 - \frac{\alpha}{2}\right) (p_i - \pi_w^+(n_i; \delta_+)) \right). \end{aligned}$$

Intuitively, the first optimization model penalizes more severely over-evaluations than under-evaluations of the price in order to return an under-estimator while the second model does the opposite. The connection to the notion of quantile estimation emerges when one assumes that, conditionally on observing n_i , the $\alpha/2$ -th quantile of the market price can be computed using a member of the parametric family $\pi_w^-(n_i; \delta_-)$. In this case, as N converges to infinity, then δ_- can be shown to converge in probability to the true value, and similarly in the case of δ_+ . In contrast, the method of least squares offers a similar type of convergence but towards the conditional expected value of

250

the market price. We refer interested readers to [20] for a thorough presentation of this regression
 255 scheme.

In our implementation, we model the lower and upper bounds of the supply curve with piecewise
 linear functions. For the sake of consistency with the nominal supply curve determined in Section
 2.2, the same breakpoints are used. This modeling decision also has the advantage of reducing the
 number of binary variables involved in the mixed-integer convex quadratically constrained program
 260 that is proposed in Section 3.3 to identify robust self-scheduled bids. It was however necessary to
 include an additional breakpoint at 12.817 GW in order to prevent the lower bounding function
 from returning negative prices. Negative prices are known not to occur in the New York market
 because of the way the price selection mechanism is designed. This is however not the case in all
 electricity market given that negative prices do emerge temporarily in some markets because of
 265 generators that are unwilling or unable to interrupt suddenly their output.

For completeness, we present below the resulting linear program that needs to be solved in order
 to obtain the calibrated parameters for the lower bounding function:

$$\begin{aligned}
 \min_{\delta, t, y} \quad & (1/N) \sum_{i=1}^N t_i \\
 \text{subject to} \quad & t_i \geq (1 - \frac{\alpha}{2})(y_i - p_i), \forall i = 1, \dots, N \\
 & t_i \geq \frac{\alpha}{2}(p_i - y_i), \forall i = 1, \dots, N \\
 & y_i = \sum_{j=1}^3 \delta_j (n_i - \gamma_j) \mathbf{1}\{n_i \geq \gamma_j\} \\
 & \delta \geq 0,
 \end{aligned}$$

where $\gamma_1 = 12.817$, $\gamma_2 = 25.558$, and $\gamma_3 = 28.098$ are the three breakpoints at which the piecewise
 linear function changes slope, while each δ_j captures by how much the slope increases from one
 270 piece to the other. Finally, $\mathbf{1}\{y \geq 0\}$ is the indicator function that returns one if the condition is
 satisfied and zero otherwise.

Based on the result of our calibration, we will employ in the remainder of the paper the following
 calibrated curves to capture how low and how large the market price might be when submitting a
 bid of P_t^d or P_t^c :

$$f_t^-(q_t) := \pi^-(d_t - w_t - q_t) = \pi_w^-(n_t - q_t) \quad f_t^+(q_t) := \pi^+(d_t - w_t - q_t) = \pi_w^+(n_t - q_t),$$

where

$$\pi_w^-(y) = \begin{cases} 0 & \text{if } 0 \leq y \leq \gamma_1 \\ 2.269y - 29.081 & \text{if } \gamma_1 < y \leq \gamma_2 \\ 3.508y - 60.767 & \text{if } \gamma_2 < y \leq \gamma_3 \\ 6.248y - 137.764 & \text{if } \gamma_3 < y \end{cases} \quad \& \quad \pi_w^+(y) = \begin{cases} 2.272y - 9.023 & \text{if } 0 \leq y \leq \gamma_2 \\ 3.320y - 35.820 & \text{if } \gamma_2 < y \leq \gamma_3 \\ 7.884y - 164.069 & \text{if } \gamma_3 < y. \end{cases} \quad (3)$$

The regressions (nominal, lower bound, and upper bound, detailed in equations (2) and (3), respectively) are graphed in Figure 3. Given our choice of α , we note that quantile regression guarantees our upper and lower bounds encapsulate 90% of the historical data [21]. An extremely risk averse storage operator could update the choice of α to ensure an even broader coverage of historical outliers. The main goal of these models, achieved through quantile regression, is to obtain an accurate representation of the uncertainty set for each value of net load, with this information utilized in the robust self-scheduling optimization model (see Section 3). In this work, for ease of interpretability, we model price as dependent solely on net demand. However, we acknowledge that future work could improve the explained price variance by incorporating more explanatory variables, such as solar irradiance, hydro conditions, thermal fuel prices, generator outage conditions, etc.

3. Robust formulation of the self-scheduling problem

In this section, we propose a robust optimization model for a storage facility operator that is risk-averse regarding the uncertainty in the actual market price when submitting self-scheduled bids to a day-ahead market. We review in Section 3.1 some background on the general methodology before focusing on the choices we made in this application. Next, Section 3.2 discusses how the approach presented in [22] can be used to robustify problem (1) in a way that immunizes the operator against potential daily losses. We then present in Section 3.3 how this robust problem can be reformulated as a mixed-integer convex quadratically constrained program.

3.1. Background on robust optimization

Robust optimization is a technique for optimization under uncertainty, that has received an increasing amount of interest in the last ten years. Contrary to other approaches that handle uncertainty, such as stochastic programming, it removes the need to identify a probabilistic model of

the likelihood of every possible future outcomes, replacing it with the characterization of a so-called
295 uncertainty set. In principle, the robust optimization paradigm seeks solutions that remain feasible
under any potential outcomes that fall within the prescribed uncertainty set. Its first application
to mathematical programming dates from [23] where the authors proposed that each uncertain
parameter be circumscribed to its respective interval. This approach was quickly considered overly
conservative as it allowed worst-case scenarios where all the parameters take on their extreme
300 values simultaneously. This issue was addressed in [24], where Ben-tal and Nemirovski propose
the use of ellipsoidal uncertainty sets that do not allow for such events to be considered. Even
more recently, the authors of [25] introduced a polyhedral set known as the budgeted uncertainty
which allows one to control the level of conservatism through the use of a “budget” parameter
 Γ which defines how many of the uncertain parameters are allowed to reach an extreme value.
305 These important works contributed significantly to the popularization of the method. Overall, one
might consider the following advantages that a robust optimization framework typically has over
stochastic programming:

- For many classes of optimization problems, the robust optimization formulation is computationally tractable (see [26]) while a stochastic programming approach might be confronted to
310 the challenge of performing high-dimensional integration.
- The non-probabilistic approach used in robust optimization allows the decision-maker to immunize against uncertainty without having to define a distribution for the uncertain parameters.

The latter advantage is especially practical in the case of data-driven problems, where there is no
315 particular reason to represent the random vector with a distribution of a specific form, such as
the normal distribution. In the case of stochastic programming, it is necessary to identify and
calibrate a joint distribution for the vector of uncertain parameters. This distribution defines both
the marginal likelihood of each parameter taken separately and the specifics of how each of them is
correlated to others. When the random vector is large and the observations rather limited, then it
320 can easily be the case that there are many distribution models that could explain the observations
equally well thus making this choice rather arbitrary. This difficulty has given rise to what might
be thought of as the “Optimizer’s curse” (see [27]) given that the solution that is identified by a
stochastic program can easily over-exploit the selected distribution model resulting in an optimistic

view of future performance which can lead to great post-decision disappointment.

325 For these reasons, the robust optimization approach has been applied in many different domains including power systems operations. In particular, from the market operator’s perspective, more and more sources of uncertainty have to be taken into account in the unit commitment problem. Given the increasing penetration of variable energy sources (wind, solar), and the recent development of price-responsive demand, solving this problem has become more challenging. In [28],
330 Bertsimas et al. propose a two-stage adaptive robust optimization model for the security constrained unit commitment problem in the presence of nodal net injection uncertainty. In [29], a polytopic uncertainty set is constructed to capture wind uncertainty, and is then integrated in the robust formulation of the unit commitment problem. Finally, [30] proposes a robust optimization approach to provide a robust unit commitment schedule for the thermal generators in the day-ahead
335 market that minimizes the total cost under the worst wind power output scenario. We also refer the reader to [31] and [32], where robust models are developed to optimize the long-term investment plans (both in energy storage facilities and in the transmission network expansion) that will guarantee a feasible system operation under various renewable energy output scenarios. To the best of our knowledge, there is no prior work on applying a robust optimization approach to the
340 self-scheduling problem of a storage facility operator.

3.2. The robust optimization model

When confronted to historical observation of market prices such as those studied in Section 2, it is easy to see how a storage facility operator might express some concerns regarding the implementation of a self-scheduling bid strategy that does not account for price uncertainty. In
345 particular, since supply curves are usually monotonic, it is often the case that such a “nominal strategy” would recommend to charge the battery during the lowest demand hour, and sell this electricity back when the demand is at its highest level. As seen in Figure 3, when price uncertainty is large, doing so exposes the operator to the risk that the realized market price for the period with low demand (i.e. a scheduled charge) be higher than during the period where a discharge was
350 planned, hence leading to a net financial loss. This motivates the use of a robust optimization approach that will allow the storage facility operator to control his exposure to net financial losses.

In what follows, we derive a robust optimization model based on the paradigm presented in [22] which can directly exploit the description of uncertainty that was presented in Section 2.3,

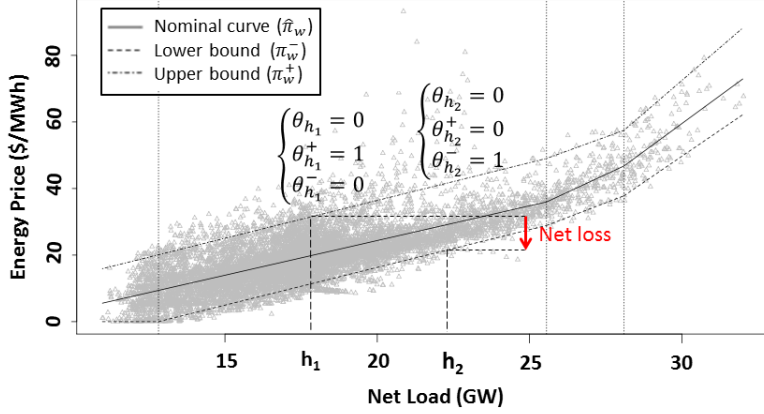


Figure 3: Situation where the nominal strategy exposes the operator to a net financial loss. The values h_1 and h_2 represent two periods with respectively low and high demand thus motivating a charge at period 1 followed by a discharge at period 2 when considering the nominal supply curve $\hat{\pi}_w$. When implementing this strategy, the operator is exposed to the risk that the realized market price coincide with the upper bound π_w^+ for period 1 and lower bound π_w^- for period 2 leading to a net loss.

defining a nominal, lower and upper bound for $f(\cdot)$. Specifically, problem (1) is modified by adding a constraint that rejects a self-scheduling strategy if it has the potential of leading to a net loss when the nominal supply curve suffers a certain level Γ of perturbation. This gives rise to the following robust self-scheduling problem:

$$\max_{\{P_t^c, P_t^d, E_t\}_{t=1}^T} \sum_{t=1}^T (P_t^d - P_t^c) \hat{f}_t(P_t^d - P_t^c) - \sum_{t=1}^T C(P_t^d + P_t^c) \quad (4a)$$

$$\text{subject to} \quad \sum_{t=1}^T (P_t^d - P_t^c) f_t(P_t^d - P_t^c) - \sum_{t=1}^T C(P_t^d + P_t^c) \geq 0, \forall (f_1, f_2, \dots, f_T) \in \mathcal{F}(\Gamma) \quad (4b)$$

$$(1b) - (1f),$$

where $\mathcal{F}(\Gamma)$ captures all supply curves that can be obtained by a Γ perturbation of \hat{f}_t , mathematically speaking

$$\mathcal{F}(\Gamma) := \left\{ (f_1, \dots, f_T) \left| \begin{array}{l} \exists (\theta, \theta^-, \theta^+) \in \mathbb{R}_+^{3T}, \quad \theta_t + \theta_t^+ + \theta_t^- = 1, \forall t \in \llbracket 1, T \rrbracket \\ \sum_{t=1}^T \theta_t^- + \theta_t^+ \leq \Gamma \\ f_t(\cdot) = \theta_t \hat{f}_t(\cdot) + \theta_t^- f_t^-(\cdot) + \theta_t^+ f_t^+(\cdot), \forall t \in \llbracket 1, T \rrbracket \end{array} \right. \right\}.$$

In a language similar to the one used by the authors of [25], one can interpret Γ as the maximum number of time periods during which the supply curve is allowed to reach either of the two supply curve bounds π_w^- or π_w^+ that were identified using the historical data. One might also recognize that in the construction of $\mathcal{F}(\Gamma)$, we model for each time period t a triplet $(\theta_t, \theta_t^-, \theta_t^+)$ that will let the market price at period t take on any convex combination of $f_t^-(\cdot)$, $\hat{f}_t(\cdot)$, and $f_t^+(\cdot)$. Furthermore, when $\Gamma = 0$, problem (4) reduces to the nominal problem (1) since in this case all $(\theta_t, \theta_t^+, \theta_t^-) = (1, 0, 0)$ leading to $\mathcal{F}(\Gamma) = \{\hat{f}(\cdot)\}$. Alternatively, when $\Gamma = T$, constraint (4b) reduces to

$$\sum_{t: P_t^d \geq P_t^c} (P_t^d - P_t^c) f_t^-(P_t^d - P_t^c) - \sum_{t: P_t^d < P_t^c} (P_t^d - P_t^c) f_t^+(P_t^d - P_t^c) - \sum_{t=1}^T C(P_t^d + P_t^c) \geq 0,$$

which effectively assumes that the market price always end up being the most unfavorable with respect to the self-scheduling strategy.

It is also possible to interpret the robust constraint (4b) as an approximation of the following chance constraint:

$$\mathbb{P}\left(\sum_{t=1}^T (P_t^d - P_t^c) \tilde{f}_t(P_t^d - P_t^c) - \sum_{t=1}^T C(P_t^d + P_t^c) \geq 0\right) \geq 1 - \varepsilon,$$

where $\tilde{f}_t(\cdot)$ is the random mapping that is assumed to have produced the historical price observations, and $\varepsilon \in [0, 1]$ characterizes the amount of probability with which we are comfortable that the constraint might not be respected. Based on the definition of $\mathcal{F}(\Gamma)$, it is possible to evaluate the probability that the historical observation of market price be a member of our uncertainty set :

$$\mathbb{P}(\tilde{f} \in \mathcal{F}(\Gamma)) \approx (1/N) \sum_{i=1}^N \mathbf{1}\{\exists f \in \mathcal{F}(\Gamma), p_t = f_t(0), \forall t\},$$

where we count what is the proportion of historical observations for which the observed price could be a result of evaluating one of the functions in $\mathcal{F}(\Gamma)$ at zero (given that the contribution of the battery facility was null historically). Figure 4 presents the estimated level of protection depending on the size of Γ . This approach can give the decision-maker an idea of the value of Γ to use depending on the level of protection needed. However, it leads to an overly conservative choice of Γ . We follow a more empirical approach, which consists in experimenting with different values of Γ . This will be described in Section 4.

Remark 1. *It is worth repeating the fact that in cases where the time period is too short for the battery operator to schedule both a charging and discharging of the battery, there is no need to add*

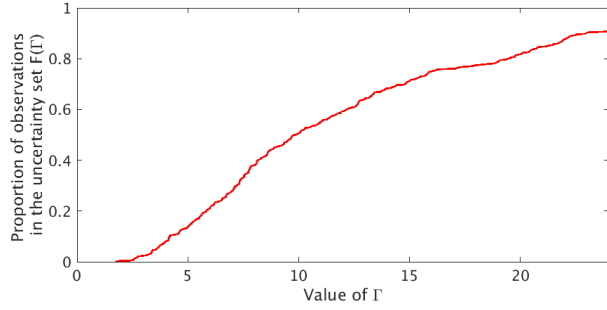


Figure 4: Chance-constraint oriented calibration of Γ

the following non-linear constraint to problem (4):

$$P_t^d P_t^c = 0, \forall t \in \llbracket 1, T \rrbracket.$$

The reason is that, as demonstrated in Appendix 6.1, problem (4) always identifies an optimal solution that satisfies this constraint.

3.3. Mixed-integer convex quadratically constrained reformulation

The robust model introduced in Section 3.1 cannot be solved using off-the-shelf solvers because it is formulated as a semi-infinite problem. To address this issue, one needs to identify a tractable reformulation for constraint (4b). To do so, we first rewrite the constraint using the following equivalent form:

$$\psi(P^d, P^c) \geq \sum_{t=1}^T C(P_t^d + P_t^c) \quad (5)$$

where

$$\psi(P^d, P^c) := \min_{(f_1, \dots, f_T) \in \mathcal{F}(\Gamma)} \sum_{t=1}^T (P_t^d - P_t^c) f_t(P_t^d - P_t^c).$$

Based on the definition of $\mathcal{F}(\Gamma)$, one can readily obtain a linear programming representation of

$\psi(P^d, P^c)$, namely:

$$\psi(P^d, P^c) = \min_{\theta, \theta^+, \theta^-} \sum_{t=1}^T \theta_t (P_t^d - P_t^c) \hat{f}_t(P_t^d - P_t^c) + \theta_t^- (P_t^d - P_t^c) f_t^-(P_t^d - P_t^c) + \theta_t^+ (P_t^d - P_t^c) f_t^+(P_t^d - P_t^c) \quad (6a)$$

$$\text{subject to} \quad \theta_t + \theta_t^+ + \theta_t^- = 1, \forall t \in \llbracket 1, T \rrbracket \quad (6b)$$

$$\sum_{t=1}^T \theta_t^- + \theta_t^+ \leq \Gamma \quad (6c)$$

$$\theta \geq 0, \theta^+ \geq 0, \theta^- \geq 0 \quad (6d)$$

Moreover, by linear programming duality, one can show that the dual problem of problem (6) takes the form:

$$\psi(P^d, P^c) = \max_{s, \lambda} \sum_{t=1}^T \lambda_t - \Gamma s \quad (7a)$$

$$\text{subject to} \quad \lambda_t \leq (P_t^d - P_t^c) \hat{f}_t(P_t^d - P_t^c), \forall t \in \llbracket 1, T \rrbracket \quad (7b)$$

$$\lambda_t - s \leq (P_t^d - P_t^c) f_t^-(P_t^d - P_t^c), \forall t \in \llbracket 1, T \rrbracket \quad (7c)$$

$$\lambda_t - s \leq (P_t^d - P_t^c) f_t^+(P_t^d - P_t^c), \forall t \in \llbracket 1, T \rrbracket \quad (7d)$$

where $\lambda \in \mathbb{R}^T$ and s are the dual variables respectively associated to constraints (6b) and (6c).

Indeed, the fact that $\psi(P^d, P^c)$ is equal to the optimum of this dual problem is guaranteed by

strong duality which applies since problem (6) is both feasible and bounded for all P^d and P^c and for all $\Gamma \geq 0$.

Given that we have obtained a representation of $\psi(P^d, P^c)$ as the optimal value of a maximization problem, one can establish that constraint (5) is equivalent to verifying whether there exists an assignment (λ, s) that satisfies constraints (7b)-(7d) and that also satisfies

$$\sum_{t=1}^T \lambda_t - \Gamma s \geq \sum_{t=1}^T C(P_t^d + P_t^c). \quad (8)$$

We can conclude that our robust optimization (4) is equivalent to:

$$\begin{aligned}
& \max_{P^d, P^c, E, \lambda, s} && \sum_{t=1}^T (P_t^d - P_t^c) \hat{f}_t(P_t^d - P_t^c) - \sum_{t=1}^T C(P_t^d + P_t^c) && (9a) \\
& \text{subject to} && (8) \\
& && (1b) - (1f) \\
& && (7b) - (7d).
\end{aligned}$$

This new formulation allows to overcome the semi-infinite nature of the original robust model. However, the nature of the resulting problem depends on the nature of the three functions $\hat{f}_t(\cdot)$, $f_t^-(\cdot)$, and $f_t^+(\cdot)$ modelling the effect of the self-scheduled bid on market price under the nominal, upper and lower supply curve. In the case that the supply curves are piecewise linear, as those constructed in Section 2, one can show that the resulting problem can be reformulated as a mixed-integer convex quadratically constrained program provided that the slope of each piece of these supply curves is non-negative. For completeness, we present below the mixed-integer convex quadratically constrained program that is equivalent to problem (4). This problem can be solved using one of several commercial solvers. We used CPLEX version 12.7 to produce the results presented in Section 4, where each run completed within a few seconds.

$$\max_{P^d, P^c, E, \lambda, s, \nu, \psi, y} \sum_{t=1}^T \psi_t - \sum_{t=1}^T C(P_t^d + P_t^c) \quad (10a)$$

$$\text{subject to } \sum_{t=1}^T \lambda_t - \Gamma s \geq \sum_{t=1}^T C(P_t^d + P_t^c) \quad (10b)$$

$$\lambda_t \leq \psi_t, \quad \forall t \in \llbracket 1, T \rrbracket \quad (10c)$$

$$\psi_t \leq \sum_{j=1}^4 -\hat{a}_j y_{tj}^2 + (n_t \hat{a}_j - \hat{b}_j) y_{tj} + n_t \hat{b}_j \nu_{tj}, \quad \forall t \in \llbracket 1, T \rrbracket \quad (10d)$$

$$\lambda_t - s \leq \sum_{j=1}^4 -a_j^- y_{tj}^2 + (n_t a_j^- - b_j^-) y_{tj} + n_t b_j^- \nu_{tj}, \quad \forall t \in \llbracket 1, T \rrbracket \quad (10e)$$

$$\lambda_t - s \leq \sum_{j=1}^4 -a_j^+ y_{tj}^2 + (n_t a_j^+ - b_j^+) y_{tj} + n_t b_j^+ \nu_{tj}, \quad \forall t \in \llbracket 1, T \rrbracket \quad (10f)$$

$$n_t - P_t^d + P_t^c = \sum_{j=1}^4 y_{tj}, \quad \forall t \in \llbracket 1, T \rrbracket \quad (10g)$$

$$\gamma_{j-1} \nu_{tj} \leq y_{tj} \leq \gamma_j \nu_{tj}, \quad \forall j = 1, \dots, 4, \quad \forall t \in \llbracket 1, T \rrbracket \quad (10h)$$

$$\sum_{j=1}^4 \nu_{tj} = 1, \quad \forall t \in \llbracket 1, T \rrbracket \quad (10i)$$

$$\nu \in \{0, 1\}^{T \times 4} \quad (10j)$$

$$(1b) - (1f),$$

where $\psi \in \mathbb{R}^T$, while the pairs of parameters (\hat{a}_j, \hat{b}_j) , (a_j^-, b_j^-) , and (a_j^+, b_j^+) respectively refer to the slopes and offsets of the j -th linear pieces of $\hat{\pi}_w(\cdot)$, $\pi_w^-(\cdot)$, and $\pi_w^+(\cdot)$. Finally, γ_1 , γ_2 , and γ_3 are the locations of the three breakpoints, while $\gamma_0 = 0$ and $\gamma_4 = \max_t n_t + P_{max}^c$. We refer the reader to Appendix 6.2 for more details on obtaining this reformulation.

4. Results and discussion

We study the case of a storage facility with 100 MW discharging and charging power and 300 MWh energy capacity (i.e. 3 hours of full power output), which is a bit more than the size of the largest battery project brought online so far [2]. For both charging and discharging operations, we consider a 90% efficiency, and a \$1/MWh variable cost due to operation and degradation [33].

We choose a scheduling horizon of one day, namely $T = 24$, which is the minimum horizon that can be considered, since bids have to be transmitted for every hour of the subsequent day on the day-ahead market. Though longer-term horizons may allow to consider both intra- and inter-day
395 arbitrage, it appeared that, in the case of NYISO day-ahead market, most of the arbitrage value was coming from intra-day peak price differential. This is especially the case when the energy capacity considered for the storage facility is limited: in our case, only 3 hours are necessary for a full charge. This can be done daily during off-peak hours to take advantage of the peak hours.

Moreover, this shorter horizon allows to assume that the perfect forecast of future net demand
400 during each one-day period is available. This assumption is supported by the public availability of day-ahead demand forecasts from the NYISO itself [34]. Though these NYISO forecasts are not perfect, they represent the best available information. While our reliance on historical data may positively bias the calculated profits, we expect any bias should be mitigated when adjusting the risk aversion parameter included in the robust optimization model.

In Section 4.1, we analyze the different bidding strategies obtained according to the chosen
405 level of risk-aversion (namely the value of Γ). Next, Section 4.2 discusses the performance of these strategies, both in terms of expected profit and protection against risk of financial loss. Especially, this evaluation will provide the decision-maker a mean to determine a proper value of Γ . Finally, the impact of the implementation of energy storage on the market prices is investigated in Section
410 4.3.

4.1. Robust self-scheduling strategy

In this subsection, to demonstrate the importance of the robust formulation, we analyze the bidding strategy according to the level of conservatism chosen by the storage operator.

To this end, it is necessary to choose a specific day of the year. The bidding strategy indeed
415 depends on the expected price for each hour of the day, and these price forecasts are computed based on the hourly load, according to the supply curve. Thus, the bidding strategy varies with the load profile, which is different every day.

To provide a better comparison, two types of days can be distinguished according to their load profile. They lead to two different types of strategies, as we will observe further. We will see
420 that for both types of days, the nominal strategy consists in purchasing electricity to charge the storage during off-peak hours, before selling electricity and discharging the storage during peak

hours. However, this nominal strategy has to evolve when the storage operator seeks to be immune to the risk of loss. This is where the strategies for the two types of days start to be different.

The first type of day is the most common, an example of this kind can be observed in Figure 5: it corresponds to the case when the price during off-peak hours in the most adverse situation (namely, the upper curve, since the storage wants to purchase electricity during off-peak hours) is greater to the price during peak hours in the most adverse situation (namely, the lower curve, since the storage wants to sell electricity during peak hours). For this type of day, if the most adverse situation occurs (namely $(\theta_t, \theta_t^+, \theta_t^-) = (0, 1, 0)$ during the purchasing hours and $(\theta_t, \theta_t^+, \theta_t^-) = (0, 0, 1)$ during the selling hours), the storage may incur losses if the nominal strategy described previously is implemented.

The second type of day offers larger arbitrage opportunities, with a greater peak price differential. An example can be observed in Figure 6. In this case, the off-peak price in the most adverse situation is lower than the peak price in the most adverse situation. Thus, the storage operator is guaranteed to make a profit when implementing the nominal strategy, even in the most adverse situation.

We may now analyze the bidding strategies observed according to the level of conservatism (specified by the value of Γ). We start with the first type of day, studying increasing integer values of Γ .

- When $\Gamma = 0$, the robust model is equivalent to the deterministic model. In this case, the optimal strategy (referred to as the nominal strategy), presented in Figure 5a, consists in charging during lowest price hours and discharge during highest price hours, and all these operations are conducted at maximum power capacity. The charging and discharging operations are concentrated during the smallest number of hours, to take advantage of the most favourable hours.
- As Γ increases, the strategy is unchanged until $\Gamma = 3$. For small budgets of uncertainty, the nominal strategy still ensures profits, even in the most adverse situations. Thus, our model allows to maintain the nominal strategy.
- For $\Gamma = 4$, the operator has to modify his strategy, to avoid being exposed to losses: the operating profit associated to the nominal strategy would be negative in the most adverse situation. The overall operational trend of the storage facility is still to charge when prices

are low and discharge when prices are high. However, the robust strategy suggests spreading the purchases and the sales over a greater number of hours, even if these hours are less favorable in terms of nominal profit (see Figure 5b). This strategy avoids being exposed to maximal deviations in the supply curve during each of the operating hours. When $\Gamma = 5$ (see Figure 5c), this trend is amplified (the purchases and sales are distributed over 7 hours and 4 hours respectively, while they were distributed over 5 hours and 3 hours with $\Gamma = 4$).

- For $\Gamma = 6$, the uncertainty is such that no strategy can guarantee positive operating profit. The optimal strategy thus consists in not operating (see Figure 5d). We understand that there is a certain value of Γ (between 5 and 6) above which the strategy will consist in not operating. We estimated empirically that this value is $\Gamma = 5.25$.

With the second type of load profile, the price differential between off-peak and peak hours is such that the nominal strategy guarantees a positive operating profit, even in the most adverse situation. Thus, the bidding strategy is the same regardless the value of Γ . This strategy is presented in Figure 6.

From this analysis, it emerges that, when a certain level of risk-aversion is reached, the robust model starts providing different bidding strategies to reduce the risk. But this reduction of the risk is done at the expense of the nominal profit: these more conservative strategies are indeed suboptimal in the nominal situation where the supply curve does not deviate from its expected position (namely $(\theta, \theta^+, \theta^-) = (1, 0, 0)$). The reduction in the nominal profit due to the risk aversion of the operator is quantified in Figure 7. To this end, we look at the profit that would have been obtained in the nominal situation with the strategies presented in figures 5a-5d. For values of Γ ranging from 0 to 3, we observed previously that the bidding strategy was unchanged. Hence, the nominal profit is also unchanged. For $\Gamma = 4$ and $\Gamma = 5$, the wider distribution of the purchases and the sales causes a slight reduction in the nominal profit. From $\Gamma \approx 5.25$, the nominal profit is zero, since the optimal strategy for this level of uncertainty is to not operate.

Figure 7 provides, for an arbitrary day of the first type, an idea of the effect of robustness on the theoretical profit obtained in the nominal situation. Although this figure corresponds to an arbitrary day, the shape of the curve would be the same for any day of the first type: the first effect of robustness (for low values of Γ) is indeed to suggest to distribute the operations, resulting in a slight decrease of the nominal profit. For greater values of Γ the most conservative strategy is

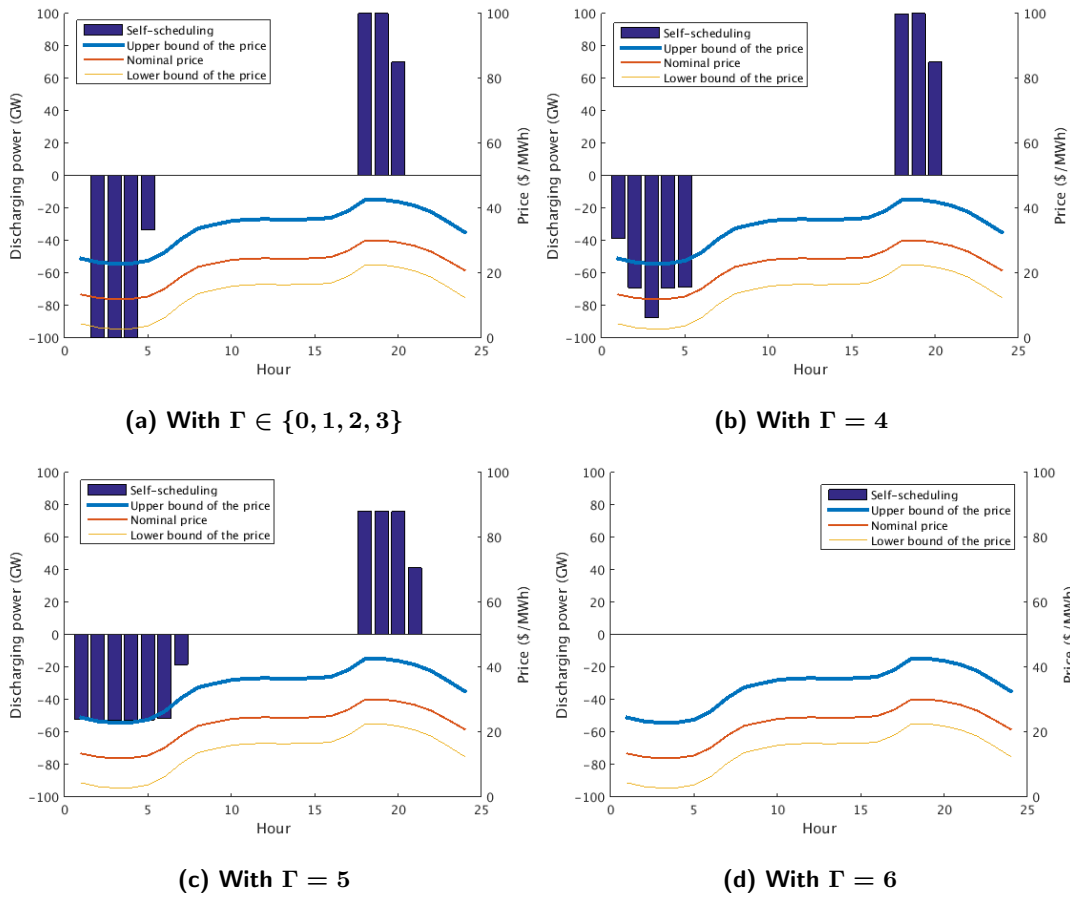


Figure 5: Self-scheduling strategy for the first type of day with varying levels of protection (Γ)

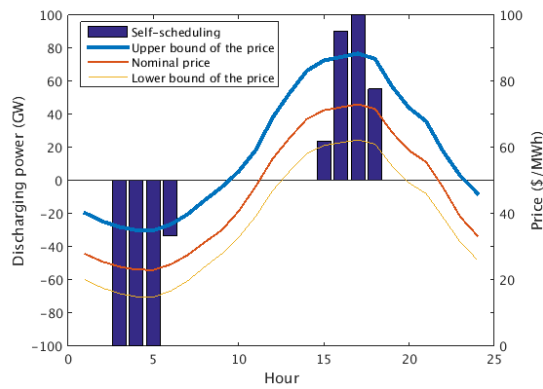


Figure 6: Self-scheduling strategy for the second type of day for all levels of protection (Γ)

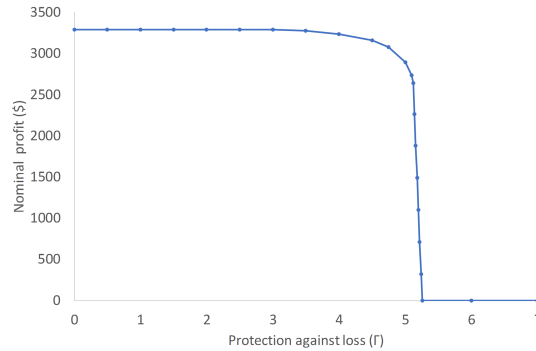


Figure 7: Nominal profit for different levels of risk-aversion

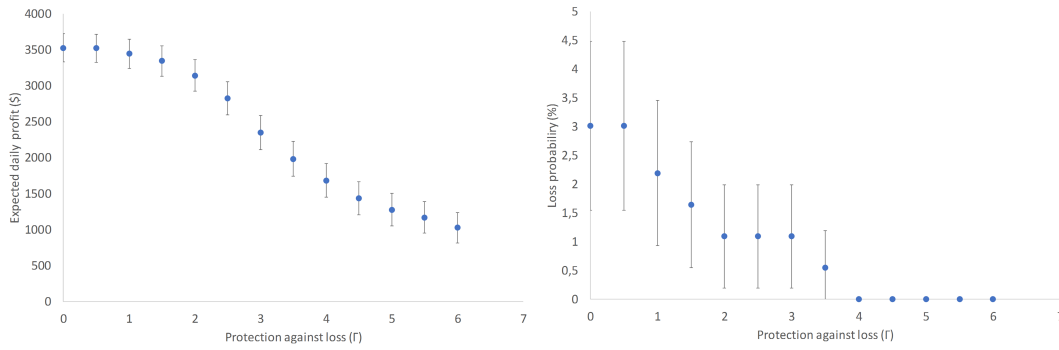
suggested (namely, no operation): it leads to a zero nominal profit. The value of Γ where the robust solution switches from operating to not operating depends on the specifics of each day. However, the storage operator needs to choose a value of Γ that he will use for every day of the year. Hence it is critical to assess the effect of the choice Γ over an entire year. This can be done by applying the robust strategies obtained to real instances of the uncertain variables, to evaluate the performance of the robust model over a larger sample of realizations for $(\theta, \theta^+, \theta^-)$.

4.2. Experimental results

The sample data of year 2016 is used to test the robust strategies on different instances of the uncertain variables $(\theta, \theta^+, \theta^-)$. Our approach follows the idea introduced by Bertsimas in [25], and consists of experimenting with different values of Γ , to compare the performance of the model. It provides the decision-maker with a tool to compare, when increasing Γ , the corresponding loss in the expected profit with the related increase in robustness. This empirical approach is different from the chance-constraint approximation introduced in Section 3.3, and will be privileged.

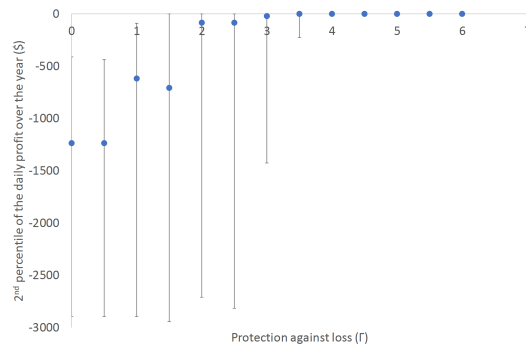
We understand that the choice of Γ corresponds to a tradeoff between the expected profit and the risk. The risk is evaluated using two different metrics: the probability to incur losses, and the “worst-case” profit (represented by the 2nd percentile of the profits obtained over the year). The results are presented in Figures 8, where the 90% confidence interval is presented.

Figure 8a shows that the expected profit is reduced as Γ increases: this can be referred to as the price of robustness. However, this robustness allows risk reduction, both in terms of loss probability



(a) Expected profit

(b) Loss probability



(c) Second percentile of the profit

Figure 8: Experimental study of the performance of different robust strategies (corresponding to different values of Γ) for 2016

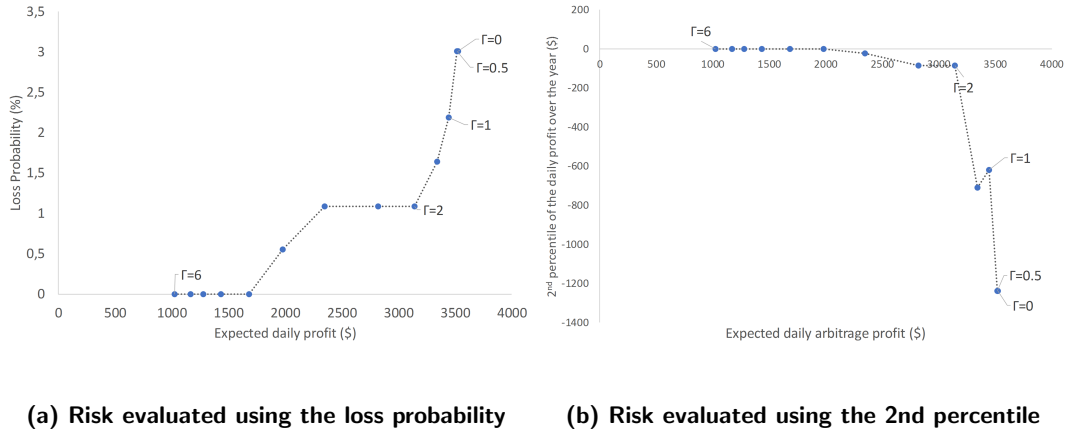


Figure 9: Trade-off between the expected profit and the risk

(see Figure 8b) and in terms of “worst-case” profit (see Figure 8c). For values of Γ greater than 4, the loss probability equals zero: the robust model allows the identification of days when operating is too risky.

These figures highlight the necessity of finding a compromise between expected profit and risk. The objective of the decision-maker is to find a value of Γ for which the expected profit is not curtailed too much with respect to the deterministic model, while reducing risk. Figure 9 illustrates this tradeoff, representing simultaneously the experimental value achieved for both objective (expected profit and risk management). It appears that, in the case of $\Gamma = 2$, the risk is significantly reduced, both in terms of loss probability (1.09% loss probability compared with 3.01% with the nominal strategy) and “worst-case” profit (\$ -83.94 versus \$ -1237.54), while the expected profit remains reasonably high (\$3143 compared with \$3525 using the nominal strategy).

Therefore, $\Gamma = 2$ would be a reasonable choice for the storage operator. Figures 10a and 10b present the results that would have been obtained for year 2016 for a storage facility operating using $\Gamma = 2$. Figure 10a shows the weekly profits obtained: we notice that the highest profits are reached during the summer, which is as expected for the summer-peaking system of New York state. Indeed, 49% of the profits are realized between the 1st of June and the 31st of August. Moreover, the general daily price profile observed in figures 5 and 6 leads the storage facility to charge during the night (generally between 12 a.m. and 7 a.m.) and to discharge during the evening (mainly between 4 p.m. and 10 p.m.). Despite the choice to be immunized against risk using $\Gamma = 2$, the

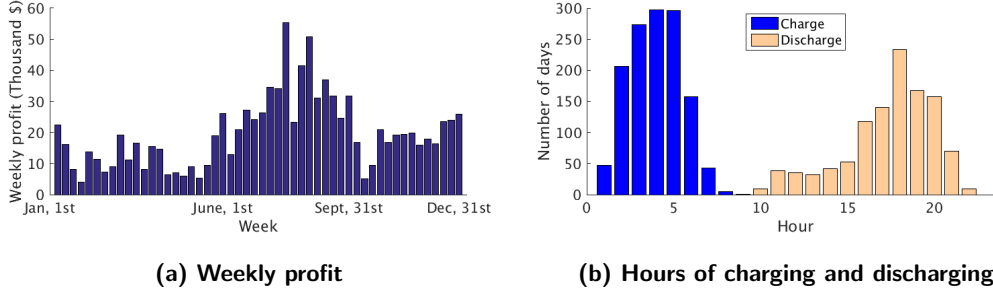


Figure 10: Storage operation for 2016, $\Gamma = 2$

520 storage activity is significant, with more than 300 days of operation in 2016.

4.3. Impact of storage operation on the market

The impact of storage operation on the price was incorporated into the self-scheduling problem to avoid over-estimating the potential arbitrage profits for a large storage facility. This formulation allows to investigate the overall impact of the storage implementation on the prices. This may be especially interesting from the perspective of the market operator.

Though the size of the energy storage facility considered in the study is comparable to the biggest existing size for a battery system, it is still marginal with respect to the size of the market (the charging and discharging power considered is equivalent to 0.3% of the highest load in New-York state). It might be of interest to study the price impacts of the storage for greater sizes. The highest sizes considered in this section are not realistic for a single energy storage facility, but this may be seen as an approximation of the implementation of several storage facilities on the market, assuming that these facilities are operated simultaneously by the same player. With the federally mandated changes in market participation of storage [3], we anticipate similarly large storage players in the near future.

535 Tables 1 and 2 present respectively the impact of differently-sized storage on the prices during charging and discharging hours. The storage facilities are assumed to be scheduled using $\Gamma = 2$.

As expected, we notice that the storage operation reduces the price differential between off-peak hours (the discharging hours in Table 1) and peak hours (the charging hours in Table 2). During discharging operations, the energy storage facility causes a significant decrease in the average price, ranging from 0.67% to 4.54% depending on the size of the storage. During charging operations, the relative increase in the price varies from 1.30% to 11.25%.

Size (% of the market)	Size (GW)	No. hours discharging	Price average (\$/MWh)		Average Price Change	
			Without	With	(\$/MWh)	%
0.3	0.1	1086	28.79	28.59	-0.19	-0.67
1	0.3	1458	27.80	27.38	-0.42	-1.52
2	0.6	1885	27.17	26.56	-0.61	-2.25
5	1.5	2403	26.97	26.02	-0.95	-3.53
10	3	2626	27.27	26.03	-1.24	-4.54

Table 1: Average price comparison without and with storage during discharging hours for different sizes of storage ($\Gamma = 2$)

Size (% of the market)	Size (GW)	No. hours charging	Price average (\$/MWh)		Average Price Change	
			Without	With	(\$/MWh)	%
0.3	0.1	1313	12.33	12.49	0.16	1.30
1	0.3	1465	12.36	12.77	0.42	3.40
2	0.6	1698	12.56	13.24	0.68	5.40
5	1.5	1956	13.19	14.33	1.15	8.71
10	3	2035	13.49	15.01	1.52	11.25

Table 2: Average price comparison without and with storage during charging hours for different sizes of storage ($\Gamma = 2$)

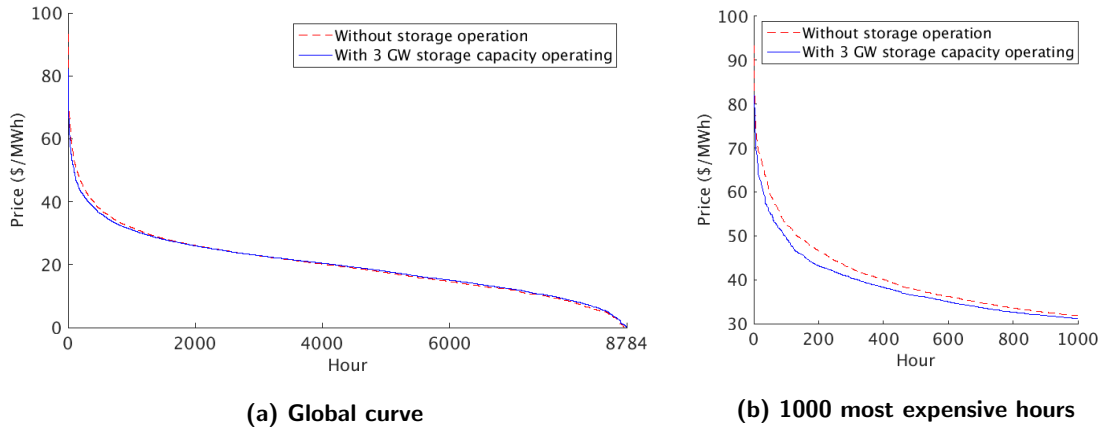


Figure 11: Price duration curve for 2016 with and without storage

We may also notice that the number of hours of operation, both charging and discharging, increases with the size of storage. This is due to the integration of the price-maker effect in the self-scheduling. When the storage size increases, it is sometimes better to distribute the purchases and sales over more hours to avoid reducing too much the peak price differential.

Figure 11 presents the price duration curves without storage and with the largest storage for the year 2016. For the sake of clarity, the duration curves obtained with other sizes for the storage facility are not represented. Especially, for smaller sizes, the resulting curve is closer to the original curve (with no storage in operation). Figure 11 allows to measure the overall impact of storage on the prices for all the hours of the year. We notice that the presence of storage slightly reduces the volatility of the prices, lowering the highest prices and increasing the lowest prices. A focus on the 1000 first hours of the price duration curve (see Figure 11b) provides a more accurate overview of the impact during the most expensive hours of the year. The presence of storage allows to lower the maximal price by 12% (from 93.23\$/MWh to 82.12\$/MWh).

Tables 3 and 4 present respectively the impact of storage operation on the price during discharging and charging hours, for the maximal size of storage. We notice that the number of operating hours decreases when the risk-aversion increases. This result may be surprising, since we observed that risk aversion led the operator to distribute his purchases and sales over a larger time window. However, the increasing level of risk-aversion concurrently reduces the number of days when the storage is operating, to avoid incurring losses. The decrease in the number of operating hours is

Gamma	No. hours discharging	Price average		Average Price Change	
		(\$/MWh)		(\$/MWh)	%
		Without	With		
0	3562	25.42	23.55	-1.87	-7.35
1	3383	25.69	24.06	-1.64	-6.37
2	2626	27.27	26.04	-1.24	-4.54
3	1538	31.26	29.97	-1.29	-4.13
4	928	36.23	34.84	-1.38	-3.82
5	630	39.55	38.16	-1.39	-3.51

Table 3: Average price comparison without and with storage during discharging hours for different values of Γ

Gamma	No. hours charging	Price average		Average Price Change	
		(\$/MWh)		(\$/MWh)	%
		Without	With		
0	2377	13.26	15.03	1.77	13.36
1	2302	13.27	15.03	1.76	13.26
2	2035	13.49	15.01	1.52	11.25
3	1427	14.55	15.92	1.37	9.45
4	938	16.42	17.8	1.38	8.39
5	666	17.6	18.94	1.34	7.62

Table 4: Average price comparison without and with storage during charging hours for different values of Γ

explained by this second effect.

Tables 3 and 4 both show that the impact of storage on the price is limited when the risk aversion of the storage increases. The increase during the charging hours drops from 13.36% for $\Gamma = 0$ to 7.62% for $\Gamma = 5$, while the decrease during the discharging hours drops from 7.35% for $\Gamma = 0$ to 3.51% for $\Gamma = 5$. This is due to the conservative strategies, which imply lower charging and discharging power, because of the distribution of purchases and sales.

5. Conclusion

This paper proposes an original approach to determine the optimal bidding strategy of a large energy storage facility doing arbitrage in a context of price uncertainty. A robust optimization framework is proposed to deal with price uncertainty. This framework is based on a representation of the market supply curve that integrates the impact of storage operation on market prices. Specifically we model the supply curve as a function of net demand, i.e., load minus wind production, as a mean to explain the variance in price while maintaining an interpretable representation. Using quantile regression to model the uncertainty bounds on the price per level of net demand, we can guarantee that 90% of the variation in price is captured in the uncertainty set. A more risk-averse storage operator could opt for an even more inclusive representation of variations.

The robust optimization formulation integrates the risk aversion of the energy storage operator with respect to financial loss through the operator's choice of a budget of uncertainty Γ . This allows a broad variety of strategies to be implemented, according to the magnitude of the budget with which the operator is comfortable. The nominal strategy (i.e. $\Gamma = 0$) consists in benefiting from the lowest (respectively highest) demand hours to charge (respectively discharge) the battery with high power output. As the level of risk aversion increases, the general trend is then to distribute the storage operations over an increasing range of time steps to avoid being impacted by a maximal perturbation at each hour of operation. Though greater values of Γ provide more conservative strategies, thus lower expected profits, they result in a decrease in terms of risk exposure. A good compromise between these two objectives is reached using $\Gamma = 2$: the loss probability is thus lowered from 3.01% to 1.09%, while the expected profit is reduced by only 10.80% with respect to the nominal strategy.

Finally, we assess the overall impact of energy storage market participation on price. It is found that larger energy storage facilities can provoke a great increase in off-peak prices (up to 13.36% for zero risk-aversion operators) and a great decrease in peak prices (up to 7.35%). This effect is mitigated when the storage operator is risk averse.

In closing, we point out that the issues relating to the location of the storage facility was not addressed. To evaluate the actual profits of the storage facility, transmission costs should be incorporated in the self-scheduling model. The representative supply curves and the developed robust model could be used in future work to formulate an optimization framework to find the optimal location for the storage facility.

6. Appendix

6.1. *Optimal solutions to problems (1) and (4) satisfy $P_t^d P_t^c = 0$*

In this appendix, we demonstrate that the set of optimal solutions for problems (1) and (4) necessarily satisfy the constraint:

$$P_t^d P_t^c = 0, \forall t \in \llbracket 1, T \rrbracket. \quad (11)$$

600 The main part of this demonstration consists of the following proposition.

Proposition 1. *Let the tuple $\{(P_t^d, P_t^c, E_t)\}_{t=1}^{T+1}$ be any solution that satisfies (1b)-(1f) but not (11), then there exists a solution $\{(\bar{P}_t^d, \bar{P}_t^c, \bar{E}_t)\}_{t=1}^{T+1}$ that satisfies (1b)-(1f) and (11), and achieves strictly greater performance with respect to*

$$\psi(\{(P_t^d, P_t^c)\}_{t=1}^T) := \sum_{t=1}^T (P_t^d - P_t^c) f_t(P_t^d - P_t^c) - \sum_{t=1}^T C(P_t^d + P_t^c) \quad (12)$$

for any choice of $\{f_t\}_{t \in \llbracket 1, T \rrbracket}$ such that each f_t is non-negative and non-increasing and for any $C > 0$.

Proof. Let us consider an assignment $\{(P_t^d, P_t^c, E_t)\}_{t=1}^{T+1}$ that satisfies (1b)-(1f) but not (11). Our proof decomposes in two steps. We first show that given any initial choice for \bar{E}_1 such that $\bar{E}_1 \in$
605 $[E_1, E_{\max}]$, we can construct an assignment for $\{\bar{P}_t^d\}_{t=1}^T, \{\bar{P}_t^c\}_{t=1}^T, \{\bar{E}_t\}_{t=2}^{T+1}$ that satisfies constraints (1b)-(1e) and (11), and achieves a strictly larger value according to ψ . We then confirm that it is always possible to identify a $\bar{E}_1 \in [E_1, E_{\max}]$ for which this constructed assignment also satisfies (1f).

Step 1: Given any initial reference battery charge $\bar{E}_1 \in [E_1, E_{\max}]$, for any time step $t = 1, \dots, T$, we construct the following candidate solution

$$\bar{P}_t^d := \begin{cases} P_t^d - P_t^c & \text{if } P_t^d \geq P_t^c \\ 0 & \text{otherwise} \end{cases} \quad (13)$$

$$\bar{P}_t^c := \begin{cases} \min\left(P_t^c - \frac{1}{\eta^2} P_t^d; \frac{1}{\eta}(E_{\max} - \bar{E}_t)\right) & \text{if } P_t^d \leq \eta^2 P_t^c \\ 0 & \text{otherwise} \end{cases} \quad (14)$$

$$\bar{E}_{t+1} := \bar{E}_t + \eta \bar{P}_t^c - \frac{1}{\eta} \bar{P}_t^d \quad (15)$$

We start by highlighting a few properties of the constructed $\{(\bar{P}_t^d, \bar{P}_t^c, \bar{E}_t)\}_{t=1}^{T+1}$. In particular, since $P_t^d \geq 0$ and $P_t^c \geq 0$ it is clear from their definitions that for all t , $\bar{P}_t^d \leq P_t^d$ and $\bar{P}_t^c \leq P_t^c$. Given that $\{P_t^d\}_{t=1}^T, \{P_t^c\}_{t=1}^T$ does not satisfy (11), there must also exist a \bar{t} , such that both $P_{\bar{t}}^d > 0$ and $P_{\bar{t}}^c > 0$ thus we have that

$$\bar{P}_{\bar{t}}^d \leq \max(0, P_{\bar{t}}^d - P_{\bar{t}}^c) < P_{\bar{t}}^d \quad \bar{P}_{\bar{t}}^c \leq \max(0, P_{\bar{t}}^c - P_{\bar{t}}^d) < P_{\bar{t}}^c.$$

Furthermore, one can establish that $\bar{E}_t \geq E_t$ recursively from $t = 1$ to $t = T + 1$. Of course, for $t = 1$ this is the case based on how \bar{E}_1 was initialized. Next, assuming that $\bar{E}_t \geq E_t$, we can inductively show that it is also the case that $\bar{E}_{t+1} \geq E_{t+1}$ for each of the three possible scenarios. If $P_t^d \geq P_t^c$, then

$$\bar{E}_{t+1} = \bar{E}_t - \frac{1}{\eta}(P_t^d - P_t^c) \geq E_t + \frac{1}{\eta}P_t^c - \frac{1}{\eta}P_t^d \geq E_t + \eta P_t^c - \frac{1}{\eta}P_t^d = E_{t+1},$$

since $\eta \in]0, 1]$. Alternatively, if $P_t^c \geq P_t^d \geq \eta^2 P_t^c$, then

$$\bar{E}_{t+1} = \bar{E}_t \geq E_t \geq E_t + \eta P_t^c - \frac{1}{\eta}P_t^d = E_{t+1},$$

since $\eta^2 P_t^c - P_t^d \leq 0$. Thirdly, when $P_t^d \leq \eta^2 P_t^c$, we have that

$$\begin{aligned} \bar{E}_{t+1} &= \bar{E}_t + \eta \min\left(P_t^c - \frac{1}{\eta^2}P_t^d; \frac{1}{\eta}(E_{\max} - \bar{E}_t)\right) \\ &= \min\left(\bar{E}_t + \eta P_t^c - \frac{1}{\eta}P_t^d; E_{\max}\right) \\ &= \min\left(E_t + \eta P_t^c - \frac{1}{\eta}P_t^d; E_{\max}\right) \geq E_{t+1}, \end{aligned}$$

since both terms in the minimum operator are larger or equal to E_{t+1} .

We can then exploit these properties to confirm that all constraints (1b)-(1e) are satisfied. We already see that (1d) is satisfied by construction of the tuple. Next, we can look at (1e) and realize that $\bar{E}_t \geq 0$ follows directly from the property that $\bar{E}_t \geq E_t$. To show that $\bar{E}_t \leq E_{\max}$ we need to be more careful and proceed iteratively from $t = 1$ to $t = T + 1$. For $t = 1$, this follows from $\bar{E}_1 \leq E_{\max}$. Following the argument that $\bar{E}_t \leq E_{\max}$, we further confirm by induction that for $t + 1$, we have $\bar{E}_{t+1} \leq E_{\max}$ for the three possible scenarios. If $P_t^d \geq P_t^c$, then

$$\bar{E}_{t+1} = \bar{E}_t - \frac{1}{\eta}(P_t^d - P_t^c) \leq \bar{E}_t \leq E_{\max}.$$

Alternatively, if $P_t^c \geq P_t^d \geq \eta^2 P_t^c$, then

$$\bar{E}_{t+1} = \bar{E}_t \leq E_{\max}.$$

Thirdly, when $P_t^d \leq \eta^2 P_t^c$, we have that

$$\begin{aligned}\bar{E}_{t+1} &= \bar{E}_t + \eta \min \left(P_t^c - \frac{1}{\eta^2} P_t^d; \frac{1}{\eta} (E_{\max} - \bar{E}_t) \right) \\ &\leq \bar{E}_t + (E_{\max} - \bar{E}_t) = E_{\max}.\end{aligned}$$

In the case of (1b) and (1c), we can straightforwardly confirm that $\bar{P}_t^c \leq P_t^c \leq P_{\max}^c$ and $\bar{P}_t^d \leq P_t^d \leq P_{\max}^c$, while the non-negativity only need to be verified under the specific condition where each one is non-zero. Namely, for $\bar{P}_t^d \geq 0$, we only need to study the case where $P_t^d \geq P_t^c$ which is trivial since $\bar{P}_t^d = P_t^d - P_t^c \geq 0$. As of $\bar{P}_t^c \geq 0$, one needs to pay close attention to the case where $P_t^d \leq \eta^2 P_t^c$, where

$$\bar{P}_t^c = \min \left(P_t^c - \frac{1}{\eta^2} P_t^d; \frac{1}{\eta} (E_{\max} - \bar{E}_t) \right) \geq \min(0; 0) = 0,$$

610 since both terms are non-negative: $P_t^c - (1/\eta^2)P_t^d \geq 0$ and $E_{\max} - \bar{E}_t$ since $\bar{E}_t \leq E_{\max}$.

The last part of this first step consists of demonstrating that $\{(\bar{P}_t^d, \bar{P}_t^c, \bar{E}_t)\}_{t=1}^{T+1}$ achieves a strictly larger ψ value than $\{(P_t^d, P_t^c, E_t)\}_{t=1}^{T+1}$. In particular, we will show that for each $t \in \llbracket 1, T \rrbracket$, both

$$C(\bar{P}_t^d + \bar{P}_t^c) \leq C(P_t^d - P_t^c) \tag{16}$$

$$(\bar{P}_t^d - \bar{P}_t^c) f_t(\bar{P}_t^d - \bar{P}_t^c) \geq (P_t^d - P_t^c) f_t(P_t^d - P_t^c), \forall t \in \llbracket 1, T \rrbracket. \tag{17}$$

This would complete our argument given that

$$\begin{aligned}\psi(\{(\bar{P}_t^d, \bar{P}_t^c)\}_{t \in \llbracket 1, T \rrbracket}) &= \sum_{t \in \llbracket 1, T \rrbracket} (\bar{P}_t^d - \bar{P}_t^c) f_t(\bar{P}_t^d - \bar{P}_t^c) - \sum_{t \in \llbracket 1, T \rrbracket} C(\bar{P}_t^d + \bar{P}_t^c) \\ &\geq \sum_{t \in \llbracket 1, T \rrbracket} (P_t^d - P_t^c) f_t(P_t^d - P_t^c) - \sum_{t \in \llbracket 1, T \rrbracket} C(P_t^d + P_t^c) + C(P_t^d + P_t^c) - C(\bar{P}_t^d + \bar{P}_t^c) \\ &\geq \sum_{t \in \llbracket 1, T \rrbracket} (P_t^d - P_t^c) f_t(P_t^d - P_t^c) - \sum_{t \in \llbracket 1, T \rrbracket} C(P_t^d + P_t^c) + C(P_t^d - \bar{P}_t^d) + C(P_t^c - \bar{P}_t^c) \\ &> \sum_{t \in \llbracket 1, T \rrbracket} (P_t^d - P_t^c) f_t(P_t^d - P_t^c) - \sum_{t \in \llbracket 1, T \rrbracket} C(P_t^d + P_t^c) = \psi(\{(P_t^d, P_t^c)\}_{t \in \llbracket 1, T \rrbracket})\end{aligned}$$

The statement in (16) is simply due to the fact that both $\bar{P}_t^d \leq P_t^d$ and $\bar{P}_t^c \leq P_t^c$. On the other hand, the statement in (17) needs to be studied under the three possible scenarios. If $P_t^d \geq P_t^c$, then

$$(\bar{P}_t^d - \bar{P}_t^c) f_t(\bar{P}_t^d - \bar{P}_t^c) = (P_t^d - P_t^c) f_t(P_t^d - P_t^c), \forall t \in \llbracket 1, T \rrbracket.$$

Alternatively, if $P_t^c \geq P_t^d \geq \eta^2 P_t^c$, then

$$(\bar{P}_t^d - \bar{P}_t^c) f_t(\bar{P}_t^d - \bar{P}_t^c) = 0 \geq (P_t^d - P_t^c) f_t(P_t^d - P_t^c),$$

since $P_t^d - P_t^c \leq 0$ and $f_t(\cdot)$ is non-negative. Thirdly, when $P_t^d \leq \eta^2 P_t^c$, we first let $\Delta := \bar{P}_t^d - \bar{P}_t^c - P_t^d + P_t^c$ which can be shown non-negative, i.e.

$$\begin{aligned} \Delta &= \bar{P}_t^d - \bar{P}_t^c - P_t^d + P_t^c = \max\left(\frac{1}{\eta^2} P_t^d - P_t^c; \bar{E}_t - E_{\max}\right) - P_t^d + P_t^c \\ &\geq \frac{1}{\eta^2} P_t^d - P_t^c - P_t^d + P_t^c \geq 0, \end{aligned}$$

and argue that for all $t \in \llbracket 1, T \rrbracket$

$$\begin{aligned} (\bar{P}_t^d - \bar{P}_t^c) f_t(\bar{P}_t^d - \bar{P}_t^c) &\geq (\bar{P}_t^d - \bar{P}_t^c) f_t(\bar{P}_t^d - \bar{P}_t^c - \Delta) \\ &\geq (P_t^d - P_t^c + \Delta) f_t(P_t^d - P_t^c) \\ &\geq (P_t^d - P_t^c) f_t(P_t^d - P_t^c), \end{aligned}$$

where we exploited the fact that $\bar{P}_t^d - \bar{P}_t^c = -\bar{P}_t^c \leq 0$ and that $f_t(\cdot)$ is non-increasing.

615 We can therefore conclude that $\psi(\{(\bar{P}_t^d, \bar{P}_t^c)\}_{t \in \llbracket 1, T \rrbracket}) > \psi(\{(P_t^d, P_t^c)\}_{t \in \llbracket 1, T \rrbracket})$.

Step 2: We are left with the second part of this proof which consists of showing that there exists a $\bar{E}_1 \in [E_1, E_{\max}]$ that makes the constructed policy also satisfy (1f). Letting $g : [E_1, E_{\max}] \rightarrow [0, E_{\max}]$ be the function that returns \bar{E}_{T+1} based on the procedure described in (13)-(15) for some initial reference battery charge $\bar{E}_1 \in [E_1, E_{\max}]$, we can first establish that $g(\cdot)$ is a continuous function since it is the composition of T continuous functions. One can also confirm that the range of $g(\cdot)$ is $[E_1, E_{\max}]$ since we established that $\bar{E}_t \in [E_t, E_{\max}]$ hence

$$g(\bar{E}_1) = \bar{E}_{T+1} \in [E_{T+1}, E_{\max}] = [E_1, E_{\max}].$$

Hence, one can make use of the intermediate value theorem on $\psi(y) := g(y) - y$ to establish that $g(\cdot)$ has a fixed point:

$$\begin{aligned} g(E_1) \geq 0 \ \&\ \& g(E_{\max}) \leq E_{\max} \quad \Rightarrow \quad \psi(E_1) \geq 0 \ \&\ \& \psi(E_{\max}) \leq 0 \\ &\Rightarrow \quad \exists y \in [E_1, E_{\max}], \psi(y) = 0 \\ &\Rightarrow \quad \exists \bar{E}_1 \in [E_1, E_{\max}], g(\bar{E}_1) = \bar{E}_1. \end{aligned}$$

This completes our proof. □

With Proposition 1 in hand, it is possible to draw the following conclusions.

Corollary 2. *Any optimal solution to problems (1) and (4) necessarily satisfies constraint (11).*

Proof. In the case of problem (1), this claim is quite straightforward since the objective function takes directly the form of $\psi(\cdot)$ as defined in (12). Therefore, any solution candidate that does not satisfy constraint (11) is necessarily a sub-optimal solution for this problem.

In the case of problem (1), the claim is similarly demonstrated. Namely, given any candidate $\{(P_t^d, P_t^c, E_t)\}_{t=1}^{T+1}$ that is feasible, one can construct a new solution $\{(\bar{P}_t^d, \bar{P}_t^c, \bar{E}_t)\}_{t=1}^{T+1}$ that satisfies constraints (1b) - (1f) and achieves a strictly larger objective value. We can also confirm that this new candidate satisfies the robust constraint (4b) since for all $(f_1, f_2, \dots, f_T) \in \mathcal{F}(\Gamma)$, we have that:

$$\sum_{t=1}^T (\bar{P}_t^d - \bar{P}_t^c) f_t(\bar{P}_t^d - \bar{P}_t^c) - \sum_{t=1}^T C(\bar{P}_t^d + \bar{P}_t^c) > \sum_{t=1}^T (P_t^d - P_t^c) f_t(P_t^d - P_t^c) - \sum_{t=1}^T C(P_t^d + P_t^c) \geq 0$$

□

6.2. Details on obtaining reformulation (10)

In order to obtain the mixed-integer convex quadratically constrained model (10), we start by treating the objective function (9a). The same procedure should then be followed on each one of constraints (7b) - (7d). Specifically, we are seeking a mixed-integer convex quadratically constrained programming representation for the function $z\hat{f}_t(z)$ for $z \in [-P_{max}^c, n_t]$ given that \hat{f} 's domain is the non-negatives. To achieve this, we take the following steps:

$$\begin{aligned} z\hat{f}_t(z) &= z\hat{\pi}_w(n_t - z) \\ &= \max_{y \in [\gamma_0, \gamma_4] : y = n_t - z} (n_t - y) \sum_{j=1}^4 (\hat{a}_j y + \hat{b}_j) \mathbf{1}\{\gamma_{j-1} \leq y \leq \gamma_j\} \\ &= \max_{y \in \mathbb{R}^4, \nu \in \{0, 1\}^4} \sum_{j=1}^4 (n_t - y_j) (\hat{a}_j y_j + \hat{b}_j \nu_j) \\ &\quad \text{subject to} \quad \sum_{j=1}^4 y_j = n_t - z \\ &\quad \sum_{j=1}^4 \nu_j = 1 \\ &\quad \gamma_{j-1} \nu_j \leq y_j \leq \gamma_j \nu_j, \forall j = 1, \dots, 4. \end{aligned}$$

The rest follows from integrating this representation in problem (9) using an epigraph formulation.
630 One then follows with the reformulation of each constraint in (7b) - (7d). Note however that the
use of $y \in \mathbb{R}^4$ and $\nu \in \{0, 1\}^4$ can be shared among all four reformulations.

Acknowledgement

This research was supported by the NSERC Energy Storage Technology Network (NESTNet),
the Canada Research Chair program, and by an IVADO Postdoctoral Scholarship to K.R. Schell.

635 Bibliography

- [1] M. Beaudin, H. Zareipour, A. Schellenberglabe, W. Rosehart, Energy storage for mitigating
the variability of renewable electricity sources: An updated review, *Energy for Sustainable
Development* 14 (4) (2010) 302–314.
- [2] California Independent System Operator, 2016-2017 Transmission Plan (March 2017).
- 640 [3] Federal Energy Regulatory Commission (FERC), Order no. 841. electric storage participation
in markets operated by regional transmission organizations and independent system operators.,
<https://www.ferc.gov/whats-new/comm-meet/2018/021518/E-1.pdf> (February 2018).
- [4] R. Sioshansi, P. Denholm, T. Jenkin, J. Weiss, Estimating the value of electricity storage in
pjm: Arbitrage and some welfare effects, *Energy Economics* 31 (2) (2009) 269–277.
- 645 [5] US Department of Energy, Grid energy storage (2013).
- [6] H. Mohsenian-Rad, Coordinated price-maker operation of large energy storage units in nodal
energy markets, *IEEE Transactions on Power Systems* 31 (1) (2016) 786–797.
- [7] S. Shafiee, P. Zamani-Dehkordi, H. Zareipour, A. M. Knight, Economic assessment of a price-
maker energy storage facility in the alberta electricity market, *Energy* 111 (2016) 537–547.
- 650 [8] F. Teixeira, J. de Sousa, S. Faias, How market power affects the behavior of a pumped storage
hydro unit in the day-ahead electricity market?, in: *European Energy Market (EEM), 2012
9th International Conference on the, IEEE, 2012, pp. 1–6.*

- [9] R. Walawalkar, J. Apt, R. Mancini, Economics of electric energy storage for energy arbitrage and regulation in new york, *Energy Policy* 35 (4) (2007) 2558–2568.
- 655 [10] R. Sioshansi, P. Denholm, T. Jenkin, A comparative analysis of the value of pure and hybrid electricity storage, *Energy Economics* 33 (1) (2011) 56–66.
- [11] E. Drury, P. Denholm, R. Sioshansi, The value of compressed air energy storage in energy and reserve markets, *Energy* 36 (8) (2011) 4959–4973.
- [12] Y. Wang, Y. Dvorkin, R. Fernandez-Blanco, B. Xu, T. Qiu, D. Kirschen, Look-ahead bidding strategy for energy storage, *IEEE Transactions on Sustainable Energy* (2017)[doi:10.1109/TSTE.2017.2656800](https://doi.org/10.1109/TSTE.2017.2656800).
- 660 [13] J. A. Sousa, F. Teixeira, S. Faias, Impact of a price-maker pumped storage hydro unit on the integration of wind energy in power systems, *Energy* 69 (2014) 3–11.
- [14] B. Dunn, H. Kamath, J.-M. Tarascon, Electrical energy storage for the grid: A battery of choices, *Science* 334 (2011) 928 – 935.
- 665 [15] New York Independent System Operator, *Power trends 2015* (2016).
- [16] New York Independent System Operator, *NYISO markets* (2015).
- [17] V. M. Muggeo, *Segmented: an R package to fit regression models with broken-line relationships*, *R news* 8 (1) (2008) 20–25.
- 670 [18] P. Twomey, K. Neuhoff, Wind power and market power in competitive markets, *Energy Policy* 38 (7) (2010) 3198–3210.
- [19] R. Koenker, G. Bassett, Regression quantiles, *Econometrica* 46 (1) (1978) 33–50.
- [20] R. Koenker, *Quantile Regression*, *Econometric Society Monographs*, Cambridge University Press, 2005.
- 675 [21] I. Takeuchi, Q. V. Le, T. Sears, A. J. Smola, Nonparametric quantile regression, *Journal of Machine Learning Research* 7 (2005) 1001 – 1032.
- [22] E. Delage, L. Gianoli, B. Sanso, A practicable robust counterpart formulation for decomposable functions : A network congestion case study, *Operations Research* 66 (2) (2018) 535–567.

- [23] A. L. Soyster, Convex programming with set-inclusive constraints and applications to inexact linear programming, *Operations Research* 21 (5) (1973) 1154–1157.
- [24] A. Ben-Tal, A. Nemirovski, Robust convex optimization, *Mathematics of operations research* 23 (4) (1998) 769–805.
- [25] D. Bertsimas, M. Sim, The price of robustness, *Operations Research* 52 (1) (2004) 35–53.
- [26] D. Bertsimas, D. B. Brown, C. Caramanis, Theory and applications of robust optimization, *SIAM review* 53 (3) (2011) 464–501.
- [27] J. E. Smith, R. L. Winkler, The optimizer’s curse: Skepticism and postdecision surprise in decision analysis, *Management Science* 52 (3) (2006) 311–322.
- [28] D. Bertsimas, E. Litvinov, X. A. Sun, J. Zhao, T. Zheng, Adaptive robust optimization for the security constrained unit commitment problem, *IEEE Transactions on Power Systems* 28 (1) (2013) 52–63.
- [29] L. Zhao, B. Zeng, Robust unit commitment problem with demand response and wind energy, in: *Power and Energy Society General Meeting, 2012 IEEE*, IEEE, 2012, pp. 1–8.
- [30] R. Jiang, J. Wang, Y. Guan, Robust unit commitment with wind power and pumped storage hydro, *IEEE Transactions on Power Systems* 27 (2) (2012) 800–810.
- [31] R. A. Jabr, I. Džafić, B. C. Pal, Robust optimization of storage investment on transmission networks, *IEEE Transactions on Power Systems* 30 (1) (2015) 531–539.
- [32] S. Dehghan, N. Amjady, Robust transmission and energy storage expansion planning in wind farm-integrated power systems considering transmission switching, *IEEE Transactions on Sustainable Energy* 7 (2) (2016) 765–774.
- [33] A. A. Thatte, L. Xie, D. E. Viassolo, S. Singh, Risk measure based robust bidding strategy for arbitrage using a wind farm and energy storage, *IEEE Transactions on Smart Grid* 4 (4) (2013) 2191–2199.
- [34] New York Independent System Operator (NYISO), Day-ahead scheduling manual, http://www.nyiso.com/public/webdocs/markets_operations/documents/Manuals_and_Guides/Manuals/Operations/dayahd_schd_mnl.pdf (October 2017).